University Library

MINERVA ACCESS

A gateway to Melbourne's research publications

Minerva Access is the Institutional Repository of The University of Melbourne

Author/s:
Tanyi, G;Peace, D;Taha, M;Cheng, E;Dinh, XH;Ren, G;Lim, C;Mitchell, A;Unnithan, RR

Title:
A Thermally Reconfigurable Photonic Switch Utilizing Drop Cast Vanadium Oxide Nanoparticles on Silicon Waveguides

Date:
2024-07

Citation:
Tanyi, G., Peace, D., Taha, M., Cheng, E., Dinh, X. H., Ren, G., Lim, C., Mitchell, A. & Unnithan, R. R. (2024). A Thermally Reconfigurable Photonic Switch Utilizing Drop Cast Vanadium Oxide Nanoparticles on Silicon Waveguides. Advanced Photonics Research, 5 (7), https://doi.org/10.1002/adpr.202300295.

Persistent Link:
https://hdl.handle.net/11343/351030

License:
cc-by

ADVANCED PHOTONICS RESEARCH
Open Access
www.adpr-journal.com

A Thermally Reconfigurable Photonic Switch Utilizing Drop Cast Vanadium Oxide Nanoparticles on Silicon Waveguides

Gregory Tanyi, Daniel Peace, Mohammed Taha, Elliot Cheng, Xuan Hiep Dinh, Guanghui Ren, Christina Lim, Arnan Mitchell, and Ranjith R. Unnithan**

Photonic switches play a vital role in optical communications and computer networks for establishing and releasing connections of optical signals. With the growing demand for ultra-compact switches in high-speed optical computing and communications, thermally reconfigurable optical switches have gained significant attention. These switches offer simplicity, ease of fabrication, and leverage a wide range of thermo-optic materials. Silicon remains an ideal platform for making photonic devices including the switches due to its compatibility with complementary metal-oxide-semiconductor (CMOS) technology and cost-effectiveness. The article presents a drop cast sub-stoichiometric vanadium oxide (VO_{2-x}) nanoparticles combined with a silicon ridge waveguide to make a compact thermally reconfigurable optical switch with low transition temperature and accelerated phase transition. Furthermore, the design achieves high modulation depth in addition to its scalability and simplicity. This study demonstrates the potential of solution-based VO_{2-x} nanoparticles in combination with silicon waveguides for efficient optical switch design for various applications.

1. Introduction

Photonic switches are indispensable components used in both optical communications and computer networks in the establishment and release of connections for optical signals.[1] These switches enable the manipulation of light signals, allowing for efficient routing and control of information in optical communication systems. With the surge in high-speed optical computing systems and high-speed optical communications, there is a growing demand for ultra-compact optical switches.[2,3]

Traditionally, several mechanisms for switching in the optical domain have been achieved including opto-mechanical,[4,5] electro-optic,[6,7] magneto-optic,[8] and acousto-optic methods.[9] The class of optical switches where thermal energy is used to drive the operation of the device is called thermally reconfigurable optical switches. Thermally reconfigurable optical switches offer structural simplicity and ease of fabrication but generally require significant power and can be subject to thermal cross-talk.[9–12]

Silicon, as a widely-used material in the semiconductor industry offers key advantages as the platform of choice for integrated photonic devices especially switches because of its compatibility with scale up manufacturing established for metal-oxide-semiconductor (CMOS) processes.[13] Silicon-based photonic thermal switches facilitate the development of hybrid systems which combine optical and electronic functionalities on the same chip.

Traditionally, silicon-based photonic switches that can be reconfigured thermally rely on micro-ring resonators (MRR) and Mach Zender Interferometer (MZI) designs but require constant application of current in order to maintain a particular switching state.[15] Alternatively, silicon waveguides integrated with phase change materials offer an alternative non-volatile solution for reconfigurable photonic switches. The use of phase change materials (PCMs) in integrated photonic switches has garnered considerable interest, thanks to advantages such as

G. Tanyi, M. Taha, C. Lim, R. R. Unnithan
Department of Electrical and Electronic Engineering
Faculty of Engineering and Information Technology
The University of Melbourne
Parkville, VIC 3010, Australia
E-mail: gtanyi@student.unimelb.edu.au; r.ranjith@unimelb.edu.au

The ORCID identification number(s) for the author(s) of this article can be found under https://doi.org/10.1002/adpr.202300295.

© 2024 The Authors. Advanced Photonics Research published by Wiley-VCH GmbH. This is an open access article under the terms of the Creative Commons Attribution License, which permits use, distribution and reproduction in any medium, provided the original work is properly cited.

DOI: 10.1002/adpr.202300295

D. Peace
Australian Research Council Centre of Excellence for Engineered Quantum Systems & School of Mathematics and Physics
University of Queensland
Brisbane, QLD 4072, Australia

E. Cheng
Centre for Microscopy and Microanalysis
The University of Queensland, Brisbane
St Lucia, QLD 4067, Australia

X. Hiep Dinh, G. Ren, A. Mitchell
Integrated Photonics and Applications Centre
School of Engineering
RMIT University
Melbourne, VIC 3000, Australia

enhanced bandwidth, higher switching contrast, reduced footprint, decreased energy consumption, and improved structural stability. Among the PCMs, germanium-antimony-tellurium (GST) and vanadium dioxide (VO_2) stand out as preferred choices due to their exceptional bandwidth capabilities and robust structural integrity.[14] Vanadium dioxide (VO_2), is a well-known Mott material for its substantial refractive index change from $3.24 + 0.30i$ to $2.03 + 2.64i$ during its first-order transition from an insulator to a metal.[14] The phase transition in VO_2 can be triggered by thermal heating, light irradiation, or external electrical fields.[15–17]

In recent times, there has been growing interest in sub-stoichiometric vanadium oxide nanoparticles as a composite material. The sub-stoichiometric property of these nanoparticles creates intrinsic strain in the lattice structure which has been leveraged to significantly reduce the transition temperature of VO_{2-x} from 68 to ≈36 °C. This impressive characteristic is achieved with a small hysteresis and without the need for dopants. Furthermore, the non-stoichiometry of the VO_{2-x} nanoparticles results in accelerated phase transition and recovery processes due to the strain induced in the lattice structure.[18] Consequently, these nanoparticles offer an exceptional material option for the advancement of thermally reconfigurable switches, providing notable enhancements in performance capabilities and using less power.

In this manuscript, we demonstrate a photonic switch utilizing silicon ridge waveguides integrated with drop cast vanadium oxide (VO_{2-x}) nanoparticles. To fabricate the device, we first create silicon waveguides on a silicon on insulator substrate, followed by the deposition of solution-based core-shell VO_{2-x} nanoparticles using a drop cast method. In the proposed design, we achieve a modulation depth of 12 dB at the telecom wavelength (1550 nm). The switching functionality of our photonic device is achieved by thermally altering the refractive index and extinction coefficient of the VO_{2-x} nanoparticles. Notably, this study represents the first instance of leveraging solution-based core–shell VO_{2-x} nanoparticles in conjunction with simple silicon ridge waveguides for the development of an integrated photonic switch. The device has a broad operating wavelength and has been shown to operate in both the C and S optical bands.

2. Design and Fabrication

2.1. Nanoparticle Photonic Switch Concept

Figure 1a shows a schematic diagram of the designed nanoparticle switch. Initially, an input laser is directed into the silicon ridge photonic waveguide, which has the dimensions of 450 nm in width and 220 nm in height, supporting a fundamental TE mode. Positioned on the waveguide are core-shell nanoparticles composed of vanadium oxide. The switch operates in 2 states: In the OFF state, there is no external heat applied and the vanadium oxide particles are in the semiconductor phase (insulator phase). However, in the ON state, the nanoparticles are switched from the insulator to the metallic phase due to the heat from the thermal stage. The insulator-to-metal transition of the nanoparticles is accompanied by a significant change in refractive index ($3.24 + 0.30i$ in the semiconductor phase to $2.03 + 2.64i$ in the metallic phase at 1550 nm). Consequently, this substantial refractive index change in the VO_{2-x} nanoparticles results in increased light leakage from the waveguide. The diminished intensity of the light in the waveguide can be attributed to its interaction with the VO_{2-x} nanoparticles in the metallic phase with a much higher coefficient of absorption. As a result, the waveguide experiences higher optical losses.

To thoroughly analyze the photonic switch, we conducted comprehensive simulations employing the finite element

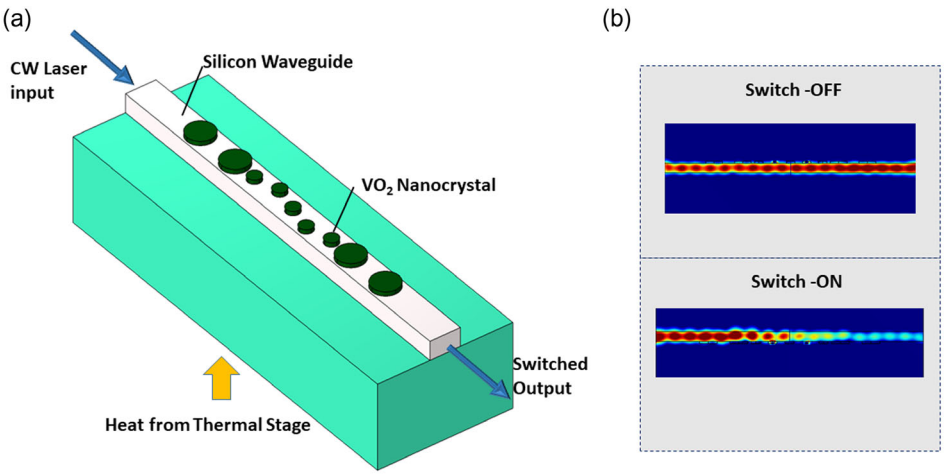

Figure 1. a) 3D schematics of the nanocrystal driven thermally reconfigurable switch with labelled components. In this sophisticated model, nanoparticles are envisioned as nanoscale disks, with their size meticulously selected to ensure that the ratio of the disk's surface area to the waveguide's surface area precisely matches the concentration of the drop-cast solution. The switching of the device is achieved by the large change in refractive index of the core–shell nanocrystals which accompanies the thermally triggered insulator to metal transition of VO_2. b) Electric field cross-sectional plots: Comparing VO_2 in semiconductor phase (Switched-Off) and metallic phase (Switched-On). The high extinction coefficient of the nanoparticles in the metallic phase reduces the intensity of light travelling through the silicon waveguide as more light is absorbed in the ON state which enables the modulation of the optical intensity.

© 2024 The Authors. Advanced Photonics Research published by Wiley-VCH GmbH

26999293, 2024, 7, Downloaded from https://onlinelibrary.wiley.com/doi/10.1002/adpr.202300295 by National Health And Medical Research Council, Wiley Online Library on [02/10/2024]. See the Terms and Conditions (https://onlinelibrary.wiley.com/terms-and-conditions) on Wiley Online Library for rules of use; OA articles are governed by the applicable Creative Commons License

method implemented in the COMSOL Multiphysics software. The simulations employed a minimum mesh size of 4 nm, while the nanoparticles were modeled with a thickness of 50 nm. The refractive indices of Si, SiO_2, and VO_2 were obtained from relevant literature sources.[19] Additionally, to accurately represent the behavior of VO_2 nanocrystals, transition boundary conditions were applied. In our simulations, the nanoparticles are modelled as nano-disks and the nanoparticle solution dilution coefficient is used to determine their coverage on the waveguide. The drop-cast solution consists of 2.7 mL of the VO_{2-x} nanoparticle solution, 600 µL of 2-butanol and an extra 600 µL of IPA to achieve a 70% solution concentration, we calculated the nanoparticles' surface area against the waveguide dimensions of 2 µm by 450 nm, utilizing four larger nanoparticles (450 nm diameter) and four smaller ones (150 nm diameter) to approximate the surface area of interaction given by the concentration of the nanoparticles. The computational domain was terminated with a top layer consisting of an 1000 µm thick air layer, and second-order scattering boundary conditions were utilized for this purpose.[1,14] These simulation parameters enabled a detailed examination of the photonic switch's performance.

2.2. Fabrication and Characterization

The device fabrication is done in two steps. In the first step, the silicon-photonic waveguides are fabricated on a commercial silicon on insulator waveguide with a 220 nm thick silicon top layer and 2 µm buried oxide layer. The fibre-to-chip gratings and waveguides are patterned using electron beam lithography (EBL; Vistec EBPG) followed by DRIE etching using a lift-off formed chromium hard-mask. The next step involves the integration of the vanadium oxide nanoparticles using the drop cast (**Figure 2**). The dispersion of the nanoparticles is achieved by using a combination of isopropyl alcohol (IPA) and 2-butanol. The solution's mixing ratios were precisely defined by combining 2.7 mL of VO_{2-x} suspended in IPA with 600 µL of 2-Butanol and further adding 600 µL of IPA, with the solution subsequently drop-casted onto the chip. Subsequently, the samples undergo a baking process to facilitate solvent evaporation (**Figure 3**).

2.3. Vanadium Oxide Nanoparticle Synthesis

To synthesize vanadium oxide nanoparticles with near room temperature insulator to metal transition, intrinsic strain is leveraged to induce structural changes in the nanoparticles. Using the scalable ambient pressure nanoparticles method, crystalline non-stoichiometric vanadium oxide particles are created from vanadium oxide hydrate precursors. The non-stoichiometric nature of the nanoparticles induces strain in the lattice-structure which leads to a more rapid insulator-to-metal transition and recovery of the nanoparticles. This approach to synthesizing vanadium oxide nanoparticles allows for a dopant-free possibility to reducing the transition temperature while also allowing for solution processing with stable precursors and allows for surface application at room temperature without the need for high temperature post annealing. **Figure 4** shows the experimentally measured optical hysteresis of the device at 1550 nm in a heating and cooling cycle from 20 to 60 °C. As can be seen from the figure, the transition temperature is 40 °C. Details of the nanoparticles synthesis and characterization are published in.[18]

3. Results and Discussion

We have fabricated two devices to investigate the switch performance in both the S band (1460–1510 nm) and C band (1535–1550 nm) using different grating coupler designs. Both grating couplers have a grating period of 685 nm with the C band optimized grating coupler having a fill factor of 0.86 and the S band grating coupler having a fill factor of 0.82. Both devices have a Si waveguides with length of 1500 um and width of 450 nm. The on-chip losses are as low as 20 dB with an additional 20 dB loss from the integration of the vanadium oxide nanoparticles on the nanowires. The device insertion loss can be further reduced by using shallow etched grating couplers that have been demonstrated to offer a superior performance.[20] Additionally, reducing the concentration of the nanoparticle dropcast solution can decrease nanoparticle density, thereby reducing the device's insertion loss.[21–49]

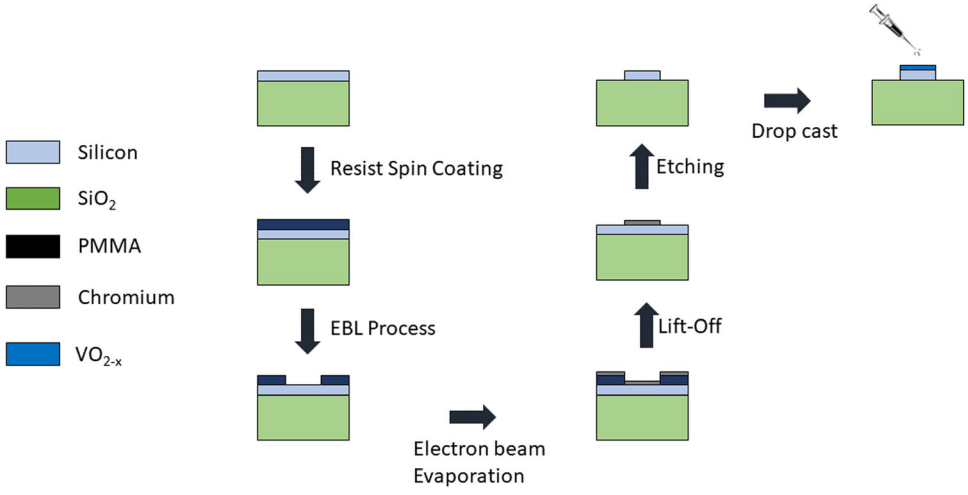

Figure 2. Illustration of the device fabrication methodology showing silicon nanowire fabrication and vanadium oxide nanoparticle deposition.

© 2024 The Authors. Advanced Photonics Research published by Wiley-VCH GmbH

26999293, 2024, 7, Downloaded from https://onlinelibrary.wiley.com/doi/10.1002/adpr.202300295 by National Health And Medical Research Council, Wiley Online Library on [02/10/2024]. See the Terms and Conditions (https://onlinelibrary.wiley.com/terms-and-conditions) on Wiley Online Library for rules of use; OA articles are governed by the applicable Creative Commons License

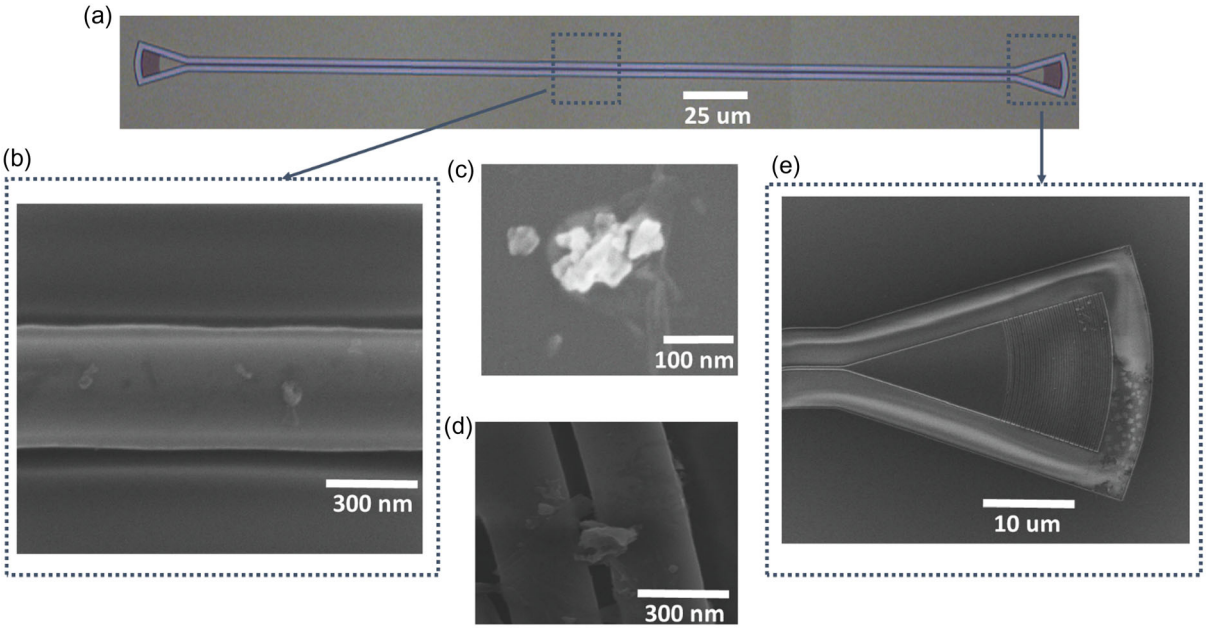

Figure 3. a) Optical micrograph of the fabricated photonic switch realized on a standard 220 nm silicon-on-insulator platform. b) Zoomed-in SEM image of the waveguide showing the vanadium oxide nanoparticles on the 450 nm wide silicon nanowire supporting a fundamental TE mode. c,d) High-resolution SEM image of the vanadium oxide nanoparticles. e) SEM image showing output grating coupler with vanadium oxide nanoparticles.

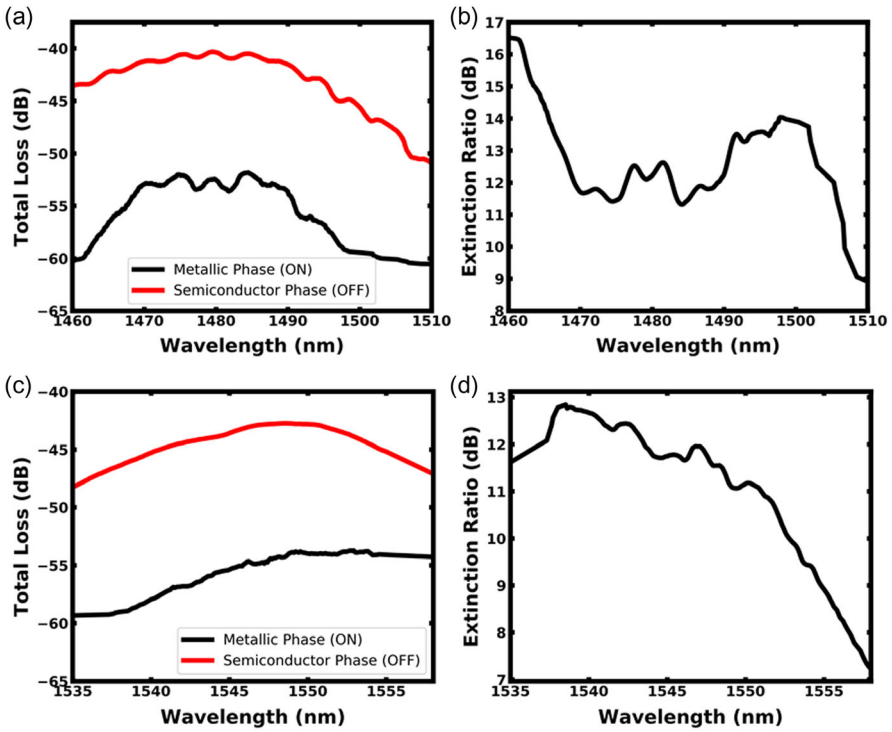

Figure 4. a) Total loss of the photonic switch in the OFF state (vanadium dioxide nanocrystals in the semiconductor phase) and in the ON state (vanadium dioxide in the metallic phase) in the S Band. b) Extinction ratio of the device in the S band (Modulation depth showing the difference in transmission of the device between the ON and OFF states c) Total loss of the photonic switch in the OFF state (vanadium dioxide nanocrystals in the semiconductor phase) and in the ON state (vanadium dioxide in the metallic phase) in the C Band d) Extinction Ratio of the device in the C band (modulation depth showing the difference in transmission of the device between the ON and OFF states.

© 2024 The Authors. Advanced Photonics Research published by Wiley-VCH GmbH

26999293, 2024, 7, Downloaded from https://onlinelibrary.wiley.com/doi/10.1002/adpr.202300295 by National Health And Medical Research Council, Wiley Online Library on [02/10/2024]. See the Terms and Conditions (https://onlinelibrary.wiley.com/terms-and-conditions) on Wiley Online Library for rules of use; OA articles are governed by the applicable Creative Commons License

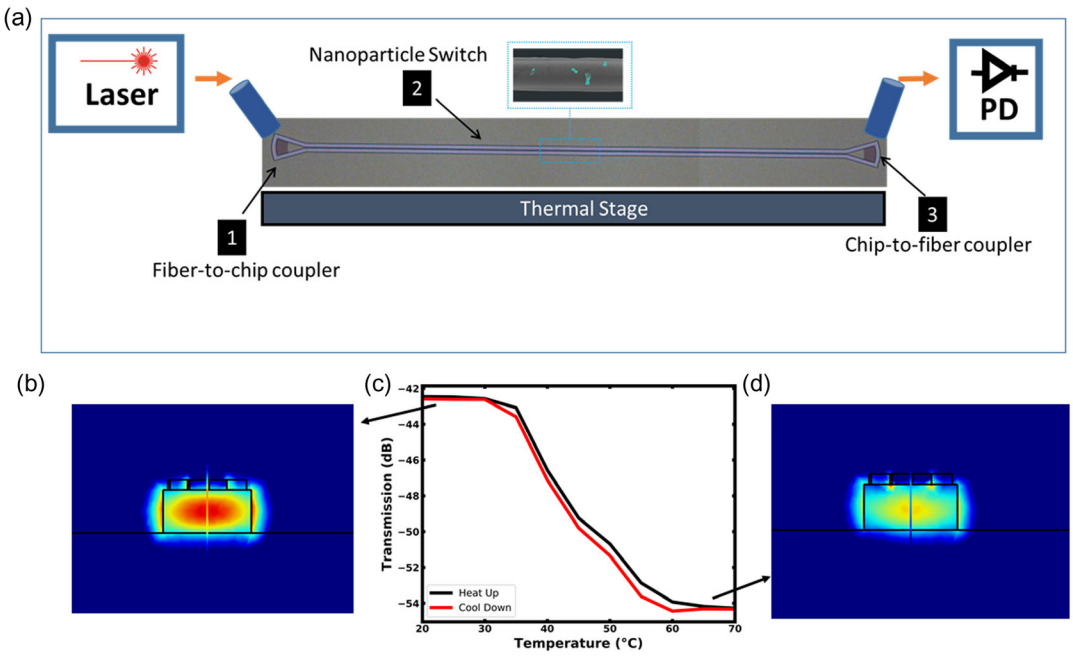

Figure 5. a) Schematic of the experimental setup used for measurement. A CW laser couples light through a single mode fibre onto the photonic chip using a directional grating coupler (Inset 1). The input light travels through the silicon nanowire with the vanadium oxide nanoparticles providing the switching functionality (inset 2). The light in the silicon ridge waveguide is then routed to the output fibre through the output chip-to-fibre grating coupler and onto a photodetector. b) A plot of the silicon waveguide showing the mode profile of the device in the OFF state. c) In situ transmittance spectra as a function of temperature at 1550 nm. d) A plot of the silicon waveguide showing the mode profile of the device in the ON state.

Figure 4b,c shows that the device has a peak extinction ratio of 13 dB in the C band and an extinction ration of up to 16.5 dB in the S band with the extinction ration ranging from 7 to 12 dB in the C band and 9 to 16.5 dB in the S band. The extinction ratio is calculated as follows: Extinction ratio = total loss (OFF State) – total loss (On State)

The range in the extinction ratio can be attributed to the variability of the VO_{2-x} extinction ratio across those wavelengths. Both devices exhibit higher optical loss in the metallic phase when external heat is applied due to the high absorption of light from the waveguide due to the interaction with the nanoparticles in their metallic phase. Both devices exhibit a broad wavelength of operation in which is limited only by the grating coupler bandwidth. These findings highlight a distinctive characteristic of the VO_{2-x} nanoparticle-based optical switches: their extensive switching range, which significantly surpasses the switching window of Ge(Si) electroabsorption modulators and free carrier silicon switches. Our current design necessitates heating the entire chip, which houses multiple devices, to trigger the phase transition of VO_{2-x}. This setup makes it challenging to estimate power consumption accurately. Also, the device's switching time is ≈20 s (corresponding to a 0.05 Hz frequency), constrained primarily by the need to heat the entire stage. In future work, we aim to incorporate localized resistive heating with electrodes near the active region to enhance modulation speed by minimizing the thermal mass affected.

The optical measurements were conducted using the setup illustrated in **Figure 5**a. A continuous-wave laser (AGILENT 8164B Lightwave) is used to optically probe the device at 1550 nm which is mounted on a thermal stage linked to a temperature controller (ILX Lightwave LDT-5412). Light from input fiber is coupled into the silicon waveguide using a fibre-to-chip coupler in which it propagates before being coupled out to the output fibre and subsequently to a photodetector using the chip-to-fiber grating coupler. Measurements of multiple devices were conducted using a custom-built motorized probing station (Newport 561-FC).

4. Conclusion

We have demonstrated a compact, thermally reconfigurable photonic switch using the drop cast vanadium oxide nanoparticles with a broad operating wavelength and a peak extinction ratio of 13 dB in the C band and 16.5 dB in the S band. This is to the best of our knowledge the first vanadium oxide nanoparticle-based thermally-reconfigurable photonic switch showing an accelerated phase transition with very little hysteresis. Owing to the broad operating wavelength of the device and scalable fabrication process, vanadium oxide nanoparticle photonic switches can pave the way to ultracompact photonic switches and modulators for optical communications.

Acknowledgements

This work was performed in part at the Melbourne Centre for Nanofabrication (MCN) in the Victorian Node of the Australian National Fabrication Facility (ANFF).

© 2024 The Authors. Advanced Photonics Research published by Wiley-VCH GmbH

26999293, 2024, 7, Downloaded from https://onlinelibrary.wiley.com/doi/10.1002/adpr.202300295 by National Health And Medical Research Council, Wiley Online Library on [02/10/2024]. See the Terms and Conditions (https://onlinelibrary.wiley.com/terms-and-conditions) on Wiley Online Library for rules of use; OA articles are governed by the applicable Creative Commons License

Open access publishing facilitated by The University of Melbourne, as part of the Wiley - The University of Melbourne agreement via the Council of Australian University Librarians.

Conflict of Interest

The authors declare no conflict of interest.

Data Availability Statement

The data that support the findings of this study are available from the corresponding author upon reasonable request.

Keywords

integrated photonics, phase change materials, silicon photonics, thermo-optics

Received: October 9, 2023
Revised: April 14, 2024
Published online: May 15, 2024

[1] Y. Li, Y. Zhang, L. Zhang, A. W. Poon, *Photonics Res.* **2015**, *3*, 4.
[2] A. F. Benner, M. Ignatowski, J. A. Kash, D. M. Kuchta, M. B. Ritter, *IBM J. Res. Dev.* **2005**, *49*, 755.
[3] A. Rahim, T. Spuesens, R. Baets, W. Bogaerts, *Proc. IEEE* **2018**, *106*, 2313.
[4] M. Spagnolo, R. Motta, R. Memeo, F. Pellegatta, A. Crespi, R. Osellame, *Opt. Express* **2020**, *28*, 23133.
[5] Pujol-Vila, F. Pujol-Vila, P. Güell-Grau, J. Nogués, M. Alvarez, B. Sepúlveda, *Adv. Funct. Mater.* **2023**, *33*, 6.
[6] R. Rajasekharan, C. Bay, Q. Dai, J. Freeman, T. D. Wilkinson, *Appl. Phys. Lett.* **2010**, *96*, 4.
[7] Z. Sun, A. Martinez, F. Wang, *Nat. Photonics* **2016**, *10*, 227.
[8] B. G. Lee, A. Biberman, J. Chan, K. Bergman, *IEEE J. Sel. Top. Quantum Electron.* **2010**, *16*, 6.
[9] L. Wan, Z. Yang, W. Zhou, M. Wen, T. Feng, S. Zeng, D. Liu, H. Li, J. Pan, N. Zhu, W. Liu, Z. Li, *Light: Sci. Applic.* **2022**, *11*, 5.
[10] R. Rajasekharan Unnithan, M. Sun, X. He, E. Balaur, A. Minovich, D. Neshev, E. Skafidas, A. Roberts, *Materials* **2017**, *10*, 383.
[11] J. Sun, R. Kumar, M. Sakib, J. B. Driscoll, H. Jayatilleka, H. Rong, *J. Lightwave Technol.* **2019**, *37*, 110.
[12] C. R. Pollock, M. Lipson, *Integr. Photonics* **2003**, *1*, 302.
[13] E. Kasper, J. Yu, *Silicon-Based Photonics* **2020**, *49*, 22.
[14] R. Mamy, A. Couget, *Solid State Commun.* **1979**, *32*, 1129.
[15] Wu, B. Wu, A. Zimmers, H. Aubin, R. Ghosh, Y. Liu, R. Lopez, *Phys. Rev. B* **2011**, *84*, 1.
[16] M. Rini, A. Cavalleri, R. W. Schoenlein, R. López, L. C. Feldman, R. F. Haglund, L. A. Boatner, T. E. Haynes, *Opt. Lett.* **2005**, *30*, 558.
[17] M. Taha, S. Walia, T. Ahmed, D. Headland, W. Withayachumnankul, S. Sriram, M. Bhaskaran, *Sci. Rep.* **2017**, *7*, 17899.
[18] G. Cocorullo, I. Rendina, *Electron. Lett.* **1992**, *28*, 83.
[19] M. Taha, S. Balendhran, P. C. Sherrell, N. Kirkwood, D. Wen, S. Wang, J. Meng, J. Bullock, K. B. Crozier, L. Sciacca, *J. Mater. Chem. A* **2023**, *11*, 7629.
[20] M. Yang, Y. Yan, Z. Wu, Y. Gu, S. Zhao, G. Morthier, M. Zhao, *Sci. Rep.* **2023**, *13*, 18112.
[21] R. Konoike, K. Suzuki, S. Namiki, H. Kawashima, K. Ikeda, *Opt. Express* **2019**, *27*, 10332.
[22] A. Joushaghani, B. A. Kruger, S. Paradis, D. Alain, J. Stewart Aitchison, J. K. S. Poon, *Appl. Phys. Lett.* **2013**, *102*, 061101.
[23] T. Jostmeier, M. Mangold, J. Zimmer, H. Karl, H. J. Krenner, C. Ruppert, M. Betz, *Opt. Express* **2016**, *24*, 17321.
[24] J. Y. Suh, E. U. Donev, R. Lopez, L. C. Feldman, R. F. Haglund, *Appl. Phys. Lett.* **2006**, *88*, 133115.
[25] C. Wan, D. Woolf, C. M. Hessel, J. Salman, Y. Xiao, C. Yao, A. Wright, J. M. Hensley, M. A. Kats, *Nano Lett.* **2021**, *22*, 6.
[26] G. Tanyi, C. Lim, R. R. Unnithan, *Nano Select* **2023**, *4*, 346.
[27] A. Youssefi, I. Shomroni, Y. J. Joshi, N. R. Bernier, A. Lukashchuk, P. Uhrich, L. Qiu, T. J. Kippenberg, *Nat. Electron.* **2021**, *4*, 326.
[28] P. Guo, R. D. Schaller, J. B. Ketterson, R. P. H. Chang, *Nat. Photonics* **2016**, *10*, 267.
[29] X. Zhang, J. Yang, *Front. Phys.* **2019**, *7*, https://doi.org/10.3389/fphy.2019.00190.
[30] K. Ishii, J. Kurumida, S. Namiki, T. Hasama, H. Ishikawa, *SPIE Proc.* **2012**, *8646*, 2.
[31] A. Schira, G. D. Valle, A. Alabastri, P. Norlander, R. Zaccharia, A. Mazzanti, *Nano Lett.* **2021**, *3*, 1354.
[32] T. Nurmohammadi, K. Abbasian, R. Yadipour, *Opt. Commun.* **2018**, *410*, 142.
[33] M. Sun, M. Taha, S. Walia, M. Bhaskaran, S. Sriram, W. Shieh, R. R. Unnithan, *Sci. Rep.* **2018**, *8*, 11106.
[34] Y. Zhang, S. Liu, W. Zhai, C. Peng, Z. Wang, J. Feng, J. Guo, *Opt. Express* **2021**, *29*, 37703.
[35] F. Gan, F. X. Kärtner, *Integr. Photonics Res. Appl./Nanophotonics* **2006**, *21*, 45.
[36] F. E. Doany, C. L. Schow, C. W. Baks, D. M. Kuchta, P. Pepeljugoski, L. Schares, R. Budd, F. Libsch, R. Dangel, F. Horst, B. J. Offrein, J. A. Kash, *IEEE Trans. Adv. Packag.* **2009**, *32*, 345.
[37] P. J. Winzer, D. T. Neilson, *J. Lightwave Technol.* **2017**, *35*, 1099.
[38] S. A. Maier, H. A. Atwater, *J. Appl. Phys.* **2005**, *98*, 36.
[39] W. L. Barnes, A. Dereux, T. W. Ebbesen, *Nature* **2003**, *424*, 824.
[40] H. A. Atwater, *Plasmonic Devices Mater.* **2005**, https://doi.org/10.21236/ada442370.
[41] H. Shi, L. Zhang, L. Wang, Z. Li, Y. Gao, Y. Wu, R. Tai, *J. Opt. Soc. Am. B* **2023**, *40*, 2365.
[42] J. Parra, J. Navarro-Arenas, M. Kovylina, P. Sanchis, *Sci. Rep.* **2022**, *12*, 974.
[43] Q. Wang, S. Zhang, C. Wang, R. Li, T. Cai, D. Zhang, *Nanomaterials* **2021**, *11*, 2988.
[44] K. Suzuki, K. Tanizawa, S. Suda, H. Matsuura, T. Inoue, K. Ikeda, S. Namiki, H. Kawashima, *Opt. Express* **2017**, *25*, 7538.
[45] D. Dai, H. Shan, L. Song, S. Wang, *SPIE Proc.* **2017**, *10242*, 51.
[46] X. Chen, J. Lin, K. Wang, *Laser Photonics Rev.* **2023**, *17*.
[47] A. Chen, E. J. Murphy, *Broadband Optical Modulators: Science, Technology, and Applications*, Vol. *1*, CRC Press, Boca Rotan **2012**, p. 278, https://doi.org/10.1201/b11444-15.
[48] Y. Xie, Y. Shi, L. Liu, J. Wang, R. Priti, G. Zhang, O. Liboiron-Ladouceur, D. Dai, *IEEE J. Sel. Top. Quantum Electron.* **2020**, *26*, 1.
[49] P. Pintus, L. Ranzani, S. Pinna, D. Huang, M. V. Gustafsson, F. Karinou, G. A. Casula, Y. Shoji, Y. Takamura, T. Mizumoto, M. Soltani, J. E. Bowers, *Nat. Electron.* **2022**, *5*, 604.

© 2024 The Authors. Advanced Photonics Research published by Wiley-VCH GmbH

26999293, 2024, 7, Downloaded from https://onlinelibrary.wiley.com/doi/10.1002/adpr.202300295 by National Health And Medical Research Council, Wiley Online Library on [02/10/2024]. See the Terms and Conditions (https://onlinelibrary.wiley.com/terms-and-conditions) on Wiley Online Library for rules of use; OA articles are governed by the applicable Creative Commons License